Nonlinearity-modulated single molecule trapping and Raman scattering analysis

Zhang, Shuoshuo; Zhang, Yuquan; Fu, Yanan; Zhu, Zheng; Man, Zhongsheng; Bu, Jing; Fang, Hui; Min, Changjun; Yuan, Xiaocong

DOI
10.1364/OE.437647

Publication date
2021

Document Version
Final published version

Published in
Optics Express

Research Article | Vol. 29, No. 20 / 27 Sep 2021 / Optics Express 32285
Optics EXPRESS

Nonlinearity-modulated single molecule trapping and Raman scattering analysis

SHUOSHUO ZHANG,[1,5] YUQUAN ZHANG,[1,5] YANAN FU,[1] ZHENG ZHU,[1,2] ZHONGSHENG MAN,[3,4] JING BU,[1] HUI FANG,[1,6] CHANGJUN MIN,[1,7] AND XIAOCONG YUAN[1]

[1]*Nanophotonics Research Center, Shenzhen Key Laboratory of Micro-Scale Optical Information Technology & Institute of Microscale Optoelectronics, Shenzhen University, Shenzhen 518060, China*
[2]*Optics Research Group, Department of Imaging Physics, Delft University of Technology, Lorentzweg 1, 2628 CJ, Delft, The Netherlands*
[3]*School of Physics and Optoelectronic Engineering, Shandong University of Technology, Zibo 255000, China*
[4]*Collaborative Innovation Center of Light Manipulations and Applications, Shandong Normal University, Jinan 250358, China*
[5]*These authors contributed equally to this work*
[6]*fhui79@szu.edu.cn*
[7]*cjmin@szu.edu.cn*

Abstract: Single molecule detection and analysis play important roles in many current biomedical researches. The deep-nanoscale hotspots, being excited and confined in a plasmonic nanocavity, make it possible to simultaneously enhance the nonlinear light-matter interactions and molecular Raman scattering for label-free detections. Here, we theoretically show that a nanocavity formed in a tip-enhanced Raman scattering (TERS) system can also achieve valid optical trapping as well as TERS signal detection for a single molecule. In addition, the nonlinear responses of metallic tip and substrate film can change their intrinsic physical properties, leading to the modulation of the optical trapping force and the TERS signal. The results demonstrate a new degree of freedom brought by the nonlinearity for effectively modulating the optical trapping and Raman detection in single molecule level. This proposed platform also shows a great potential in various fields of research that need high-precision surface imaging.

1. Introduction

Label-free single molecule detection is playing a vital role in current scientific researches, as its great applications in molecular behavior investigations and disease diagnoses at an early stage [1,2]. In these processes, a precise manipulation of molecule is always essential [3,4]. The optical tweezers technique provides an excellent alternative for this, due to its capability for non-contacting manipulation of small objects [5]. However, conventional optical tweezers are limited by the far-field diffraction and are therefore inefficient for trapping a nanometric single molecule. In contrast, surface plasmons enable the excitation of hotspot much smaller than the free-space wavelength; with this confinement, the plasmonic field facilitates trapping of various small objects with a higher precision [6,7]. For many applications, it is necessary to get stronger plasmonic field enhancement for a larger optical force to exhibit new functionalities. Nanostructures can be used to enhance the field for these scenarios. Thereinto, the gap plasmons, which are greatly enhanced and tightly confined in the narrow space between adjacent metallic structures, underlie a possible direction [8]. The local ultra-high gap plasmonic field is always much stronger than that on the surface of an isolated structure, and therefore provides a higher field gradient being conducive to the trapping forces [9,10]. The enhanced electromagnetic

#437647 https://doi.org/10.1364/OE.437647
Journal © 2021 Received 15 Jul 2021; revised 31 Aug 2021; accepted 5 Sep 2021; published 23 Sep 2021

Optics EXPRESS

field achieved due to plasmonic hybridization, meanwhile, provides an opportunity for sensitive label-free detection of Raman signals for samples located in the gap with high precision [11].

Dynamic modulation is an important requirement for molecular researches [12–14]; however, it is impossible for the nonadjustable plasmonic gaps. The controllable metallic tip-substrate configuration, typical as the tip-enhanced Raman scattering (TERS) platform [15,16], becomes an excellent alternative as it can scan the tip in three dimensions. Taking advantage of the tip-based plasmonic nanofocusing [17], it forms a hotspot with high field enhancement in the gap between the tip and substrate. The hotspot can be further optimized by the design of the excitation source, such as the use of a tightly focused vector beam [18]. Accordingly, it gives a steep intensity gradient that is beneficial for trapping [19,20], with high dynamic degrees of freedom at molecular level. Additionally, it strongly enhances the spectrographic and nonlinear optical signals of trapped samples, promoting numerous applications for qualitative and quantitative analysis [21,22]. However, maximum achievable enhancement of the hotspot is highly dependent on the physical properties of metallic structure, being limited by the charge distribution on the metal surface and also the intrinsic losses. Hence, the distribution and enhancement factor of the hotspot are always uncontrollable for linear conditions, as the physical parameters of plasmonic structure appear to be constants under a certain excitation wavelength. Differently, metallic materials can undergo an obvious nonlinear response in an external pulsed laser field [23,24], thus providing a possibility to proactively modulate their physical properties by changing the incident power.

In this work, we propose a nonlinearity-modulated single molecule trapping and enhanced Raman scattering system based on a bottom-illuminated TERS configuration. A three-dimensional finite-difference time-domain (3D FDTD) calculation is firstly carried out to get the plasmonic field distribution in the nanogap. Subsequently, the optical force exerted on a single molecule is calculated where the results reveal that the localized plasmonic gap-mode can support stable trapping at a molecular level. We consider the Kerr effect of gold tip and substrate film which can modulate both of the optical force and trapping potential simply by changing the incident power. With increased intensification factor of the field, Raman scattering enhancement factor can be effectively regulated. These results and analysis will greatly deepen and extend the nonlinear optical trapping technique and its applications in molecular analysis.

2. Results and discussion

2.1. Analytical model

Figure 1(a) shows the schematic diagram of the proposed nonlinearity-modulated single molecule trapping and enhanced Raman scattering system. A tightly focused radially-polarized laser beam is able to excite a plasmonic virtual probe with high electromagnetic enhancement on a flat gold film [25]. When a metallic tip is aligned to the virtual probe, a further enhanced plasmonic field will be generated in the nanogap between the tip and film [11]. Generally, these excitation processes also hold for pulsed cases [26,27], and plasmonic pulses are expected to play an important role in nonlinear interactions. By utilizing femtosecond pulses as excitation, a plasmonic pulsed field with high peak intensity is produced in the nanogap, providing a possibility for nonlinear modulations.

For the above system, the optical Kerr effect is the main contribution to nonlinearity. Driven by the ultra-intense gap plasmon, both the gold tip and substrate film will have a nonlinear dielectric response

$$\varepsilon = \varepsilon_l + \chi^{(3)}|\mathbf{E}_L|^2, \tag{1}$$

where $\mathbf{E}_L$ denotes the local electric field in the nanogap, $\varepsilon_l = -3.8128 + 2.3249i$ is the relative permittivity of gold under a linear excitation at the wavelength of 522 nm [28], and $\chi^{(3)} = (-76.8 + 4.3i) \times 10^{-20}$ m^2/V^2 is the third-order nonlinear susceptibility [29]. Figure 1(b) shows the nonlinear

Optics EXPRESS

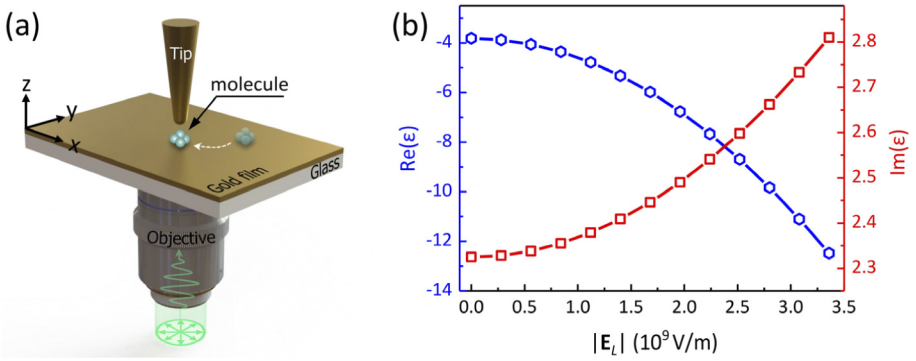

Fig. 1. (a) Schematic diagram of the nonlinearity-modulated single molecule trapping and enhanced Raman scattering system. (b) Nonlinear dielectric responses of the gold tip and substrate film to an increased electric field at 522 nm.

dielectric response of gold to an increased local electric field. As indicated by the curves, the complex permittivity can be effectively modulated when the strength of the electric field reaches 10^9 V/m, which can be easily achieved by focusing of femtosecond laser pulses. Since surface plasmon excitation needs to meet strict phase-matching condition, the change of permittivity will inevitably affect the field distribution in the nanogap and resultant optical forces.

2.2. *Nonlinearity-assistant field enhancement*

To evaluate the local electric field in the nanogap, a 3D FDTD model was built for numerical analysis. Referring to an actual experimental situation, a rounded-tip cone with an apex radius of 25 nm and a conical angle of 30° was modeled as the gold tip. According to our optimized results previously [25], the thickness of the gold film was set to 45 nm. The distance between the tip apex and the film surface was taken as 5 nm to form a nanocavity for molecule trapping. The excitation wavelength is 522 nm which is quite close to the plasmonic resonance frequency, and consequently, the plasmonic field in the nanocavity shows a relatively high electromagnetic enhancement and sensitivity to permittivity's nonlinear changes. To guarantee the numerical accuracy, a 0.4 nm mesh size was employed, and the perfectly matched layer (PML) boundary condition was used for all the simulations. Furthermore, the refractive index of the background was set to 1.33 to match the general experimental liquid conditions of optical tweezers.

Given the above analysis, the high-intensity electric field supported by the gap plasmon can induce a nonlinear response of gold nanostructures, and thereby forming a feedback mechanism that changes its own excitation. To quantify the influence of the nonlinearity, and for simplicity, we defined that $|\mathbf{E}_L|^2 = 5m \times 10^{17}$ V^2/m^2 ($m = 0, 1, 2, \ldots$) in Eq. (1), where $m = 0$ indicates a linear dielectric response and $m > 0$ corresponds to the nonlinear cases. With the FDTD model, we simulated the electric field distribution in the nanocavity configuration under different nonlinearity contributions. As illustrated in Fig. 2, the results have been normalized by the incidence $|\mathbf{E}_0|$ to give an intuitive understanding of field enhancement. It is clear that the electric field is confined in the transverse directions (< 20 nm) and limited by the gap in the vertical direction. Under the linear regime, a maximal enhancement of $\sim 4 \times 10^4$ can be realized (see Fig. 2(a)). This enhancement is due to the spatial confinement of the plasmonic field and the plasmonic hybridization between the gold tip and substrate film. It is also worth noting that the electric field shows a proportional enhancement with an increased nonlinearity, implying a process that nonlinearity makes the effective permittivity of gold closer to its plasmonic resonance. Along with the nonlinearity-assistant field enhancement, the distribution of electric field will also be slightly broadened. But according to our calculations, such dimension change is negligible for

Optics EXPRESS

a certain plasmonic nanocavity structure, and thus it will not exert impact on trapping accuracy. It can be concluded that the nonlinearity provides an alternative approach for modulating the excitation of surface plasmons without changing the excitation wavelength.

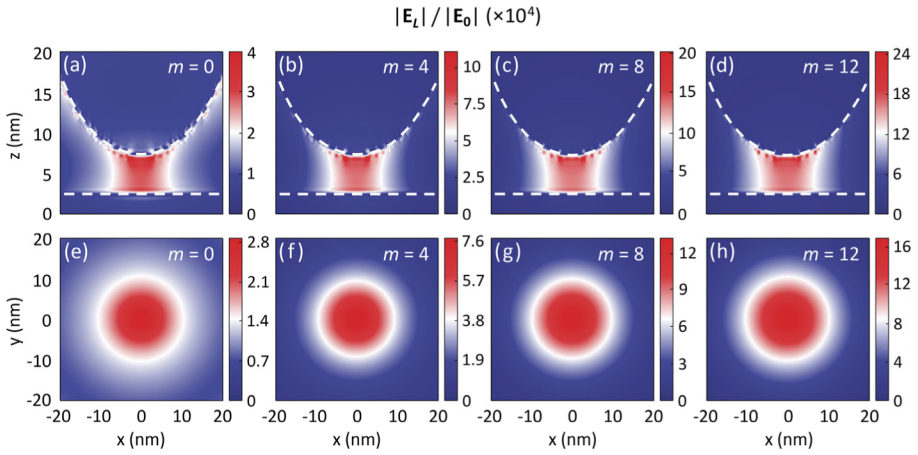

Fig. 2. Simulated local electric field enhancement in the nanocavity configuration under different nonlinearity contributions. (a)–(d) Electric field distribution in the x-z plane at y = 0. (e)–(h) Electric field distribution in the x-y plane 2 nm below the tip. *m* depicts the contribution of nonlinear effect.

2.3. Optical force and trapping potential

The exchange of momentum in electromagnetic scattering and absorption will produce an optical force for trapping and manipulating small objects. In the quasi-static limit, that is, the geometric size of the sample is much smaller than the wavelength, the time-averaged optical force and trapping potential can be written as [30,31]:

$$\langle \mathbf{F} \rangle = \frac{1}{4}\mathrm{Re}(\alpha)\nabla|\mathbf{E}_L|^2 + \frac{n_s\sigma_{ext}}{2c}\mathrm{Re}(\mathbf{E}_L \times \mathbf{H}_L^*) + \frac{\varepsilon_s\varepsilon_0 c\sigma_{ext}}{4n_s\omega i}\nabla \times (\mathbf{E}_L^* \times \mathbf{E}_L), \tag{2}$$

$$U = -\langle \mathbf{p} \cdot \mathbf{E}_L \rangle = -\frac{1}{2}\mathrm{Re}(\alpha)|\mathbf{E}_L|^2, \tag{3}$$

where α and σ_{ext} are the polarizability and extinction cross-section of the sample, respectively. n_s is the refractive index of surroundings ($n_s = 1.33$ for water), $\mathbf{E}_L$ and $\mathbf{H}_L$ are the local electric and magnetic vectors, the asterisk '*' represents a conjugate operation, c is the light speed in a vacuum, ω is the angular frequency of the electromagnetic field, ε_s is the relative permittivity of surroundings ($\varepsilon_s = n_s^2 = 1.7689$), ε_0 is the vacuum permittivity, and $\mathbf{p} = \alpha\mathbf{E}_L$ denotes the induced dipole moment.

To examine the trapping performance of our platform at the molecular level, we chose a single molecule with an equivalent radius $R = 1.25$ nm and a relative permittivity $\varepsilon_m = 4$ as the sample [32]. According to the Clausius–Mossotti relation, the molecular polarizability α is determined by [33]

$$\alpha = \alpha_0/[1 - i(2/3)k_s^3\alpha_0]; \quad \alpha_0 = 4\pi\varepsilon_s\varepsilon_0 R^3\frac{\varepsilon_m - \varepsilon_s}{\varepsilon_m + 2\varepsilon_s}, \tag{4}$$

where $k_s = n_s\omega/c$ gives the wave number in the medium. Additionally, for a small molecule ($R \ll \lambda$), the extinction cross-section is mainly contributed by its absorption part, and we should

Optics EXPRESS

therefore have [34]

$$\sigma_{ext} = k_s \cdot \mathrm{Im}(\alpha)/(\varepsilon_s \varepsilon_0). \tag{5}$$

Based on Eqs. (2)–(5), we then calculated the optical force and trapping potential exerted on the designated molecule located in the plasmonic nanocavity. Since the nanocavity is physically confined to a few nanometers in the z-direction, the longitudinal optical force $\langle \mathbf{F}_z \rangle$ is not the determinant for the trap. When the molecule is attracted to the nanocavity by the transverse optical force $\langle \mathbf{F}_{xy} \rangle$, it will inevitably stabilize at the center of the hotspot, with or without a force balance in the z-direction. Consequently, the transverse optical force is a dominant factor that tells whether a stable optical trap can be formed. Figures 3(a)–(d) show the transverse optical forces in the x-y plane (2 nm below the tip) calculated under different nonlinearity contributions. The background and black arrows give, respectively, the magnitude and direction of the optical force.

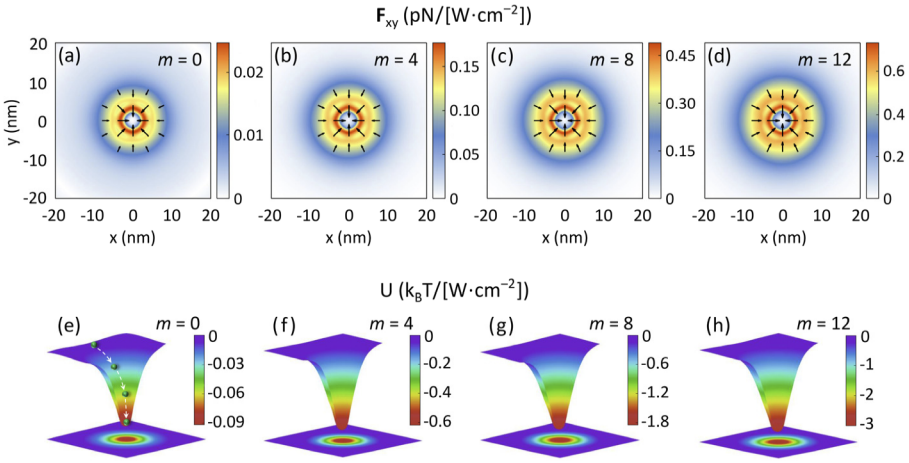

Fig. 3. (a)–(d) Calculated transverse optical forces and (e)–(h) potential wells on a single molecule located at the x-y plane (2 nm below the tip) when different nonlinearities are introduced. Here, the single molecule with an equivalent radius $R = 1.25$ nm and a relative permittivity $\varepsilon_m = 4$ can be simplified as an ideal dipole in water under the excitation at 522 nm. Both forces and potential wells are normalized by the incident optical intensity.

In this configuration, when the tip is aligned to the plasmonic virtual probe at the center, the circularly symmetrical hotspot will be more confined in a nanoscale as shown in Fig. 2. Therefore, a sharper field gradient will be achieved in this hotspot to provide a higher gradient force contributing to the trap. Meanwhile, the scattering force for a small molecule is too weak, as the extinction cross-section is proportional to the third power of molecular equivalent radius. The transverse force, as a consequence, is mainly contributed by the gradient force. It shows that the transverse force can reach a few tenths of pN/[W·cm^{-2}] in this hotspot, which is large enough for the stable trapping of a single molecule. In order to further reveal the stability, Figs. 3(e)–(h) plot the corresponding potential wells. To form a stable trap in a liquid environment, the potential well formed by gradient force must be deep enough to overcome the kinetic energy of molecule due to Brownian motion. Traditionally, an optical trap with a potential depth larger than 1 k_BT can be considered as stable, where k_B is the Boltzmann constant and T is the absolute temperature of the ambience [35,36]. As shown in Fig. 2(e), the potential depth under the linear condition is the smallest, which is ~0.09 k_BT/[W·cm^{-2}]. Accordingly, a stable trap can be realized when the incident optical intensity reaches ~11 W·cm^{-2}, a relatively low value that can be easily achieved compared to some other plasmon-based optical tweezers [37–41].

Optics EXPRESS

Due to the nonlinear optical responses of gold, in the range studied here as shown in Fig. 4, both the transverse forces and trapping potentials display a positive relationship with the excitation intensity. To show the effective contribution of nonlinearity in this process, the maximum forces and potential depths under unit incident optical intensity are plotted here. It is clear that, a stronger nonlinearity will give rise to a more stable optical trap. That is, a tunable and tight capture of molecule in the plasmonic nanocavity is feasible in such TERS based configuration. It should be noted that, both the optical force and potential depth show a slight decreasing tendency after the peak ($m = 19$). Intuitively, this can be explained by the change of permittivity relative to the plasmonic resonance, which moves to and away from the resonance condition. The electromagnetic enhancement and trapping performance (optical force and potential depth) therewith show synchronous changes. The results demonstrate that the nonlinearity provides a new degree of freedom to modulate the optical force by varying the intensity of the incident excitation beam.

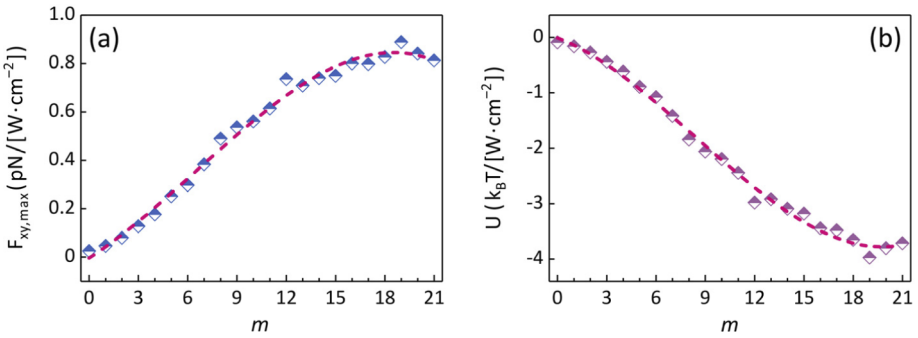

Fig. 4. Maximum optical force (a) and potential depth (b) on a single molecule located at the x-y plane (2 nm below the tip) under different system nonlinearities.

2.4. Raman enhancement factor

As discussed above, the gap plasmon can exert sufficient optical force and trapping potential on a single molecule. From another perspective, it also facilitates sensitive Raman detection due to the large electromagnetic enhancement [42,43]. In a typical TERS system, the detection sensitivity is usually characterized by a Raman enhancement factor (EF). For the proposed configuration, it is [44]

$$\mathrm{EF} = \left(\frac{I_{GPR}}{I_{VPR}} - 1\right)\frac{V_{VP}}{V_{GP}}, \tag{6}$$

where I_{GPR} and I_{VPR} are the Raman intensities measured with and without the tip, respectively, assuming that single molecule is trapped in both cases. As the Raman signal is nearly proportional to the fourth power of local electric field [45], we can rewrite Eq. (6) as

$$\mathrm{EF} \cong \left(\frac{|E_{GP}|^4}{|E_{VP}|^4} - 1\right)\frac{V_{VP}}{V_{GP}}. \tag{7}$$

In Eqs. (6) and (7), V_{GP} and V_{VP} denote the effective volumes of the gap plasmon and plasmonic virtual probe (without the tip), respectively. For small nanogaps, the field distribution is almost

Optics EXPRESS

uniform in the vertical direction. With this assumption, the effective volumes are estimated by

$$V_{GP} = h_{GP} \cdot S_{GP} = d \cdot \frac{\pi {L_{GP}}^2}{4}, \tag{8}$$

$$V_{VP} = h_{VP} \cdot S_{VP} = \delta_z \cdot \frac{\pi {L_{VP}}^2}{4}, \tag{9}$$

where L_{GP} and L_{VP} correspond to the lateral dimensions of the two plasmonic modes, which are defined by the full width at half maximum (FWHM) of electric field intensities. Here, the gap plasmon has a spatial FWHM of $L_{GP} = \mathrm{sqrt}(2rd/\varepsilon_s)$ related to the apex radius r and the gap size d [10], and $L_{VP} \approx 220$ nm is obtained from the FDTD results. δ_z is the penetration depth of the plasmonic virtual probe in the medium space above the gold film, determined by

$$\delta_z = \frac{1}{\mathrm{Im}(k_{zs})}, \tag{10}$$

with

$$k_{zs} = \frac{2\pi}{\lambda_0}\sqrt{\frac{\varepsilon_s^2}{\varepsilon + \varepsilon_s}}, \tag{11}$$

where λ_0 denotes the excitation wavelength in free-space.

To quantify the contribution of nonlinearity effect to enhanced Raman spectrum detection, EFs under different nonlinear responses are plotted in Fig. 5. The value of focused plasmonic virtual probe (without the tip) under the linear condition is employed for quantitative comparison in all cases. It shows that the nonlinearity-modulated Raman EFs are larger than that of the linear condition, and an EF as high as 10^8 can be achieved. Furthermore, the EFs show high consistency with the nonlinear field enhancement and optical force in the nanocavity, meaning that the trapping stability and Raman scattering spectrum of the trapped single molecule can be enhanced synchronously. The results indicate that it is an effective approach for precise manipulation and label-free detection of a single molecule in a tiny plasmonic nanocavity.

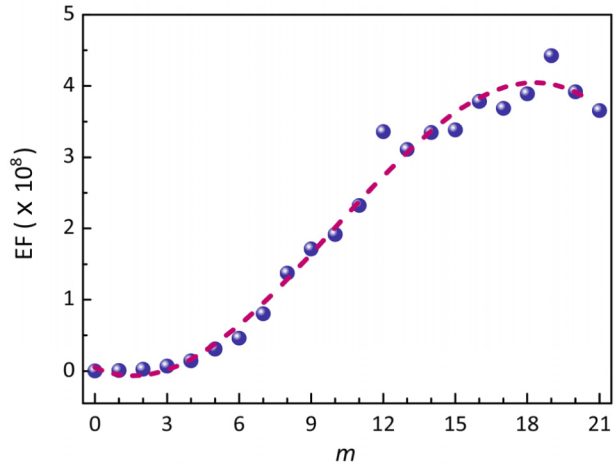

Fig. 5. Dependence of Raman enhancement factor (EF) on the nonlinear responses. The nonlinear EFs are obtained by comparison with that of the plasmonic virtual probe (without the tip) excited under the linear condition.

Optics EXPRESS

2.5. Influences of configurable parameters

In addition to the Kerr-nonlinearity, some other configurable parameters of the system, such as gap size (d), curvature radius (r), and conical angle (ϑ), will also have a certain impact on the field distribution in the nanocavity and the enhanced Raman signals of the trapped molecule. As a consequence, it is necessary to find out the influences of these parameters for further optimization. Crucial parameters are schematized in Fig. 6(a), and Figs. 6(b)–(d) depict the nonlinearity-modulated potential depths and Raman EFs of the system with different parameters. Note that only one parameter is changed at a time to avoid mixture influence between parameters. As shown in Fig. 6(b), the potential depths and Raman EFs of the system are greatly reduced when the gap size is enlarged to 10 nm. It can be seen that a smaller gap size is conducive to the molecular trapping and detection. In contrast, the impact of the curvature radius and conical angle on the system is relatively weak if the parameters are changed in a sufficiently small range, as demonstrated in Fig. 6(c) and 6(d). It is also worth mentioning that the control of the gap size in the experiment is much easier than the other two parameters, because it does not require precise processing of the tip.

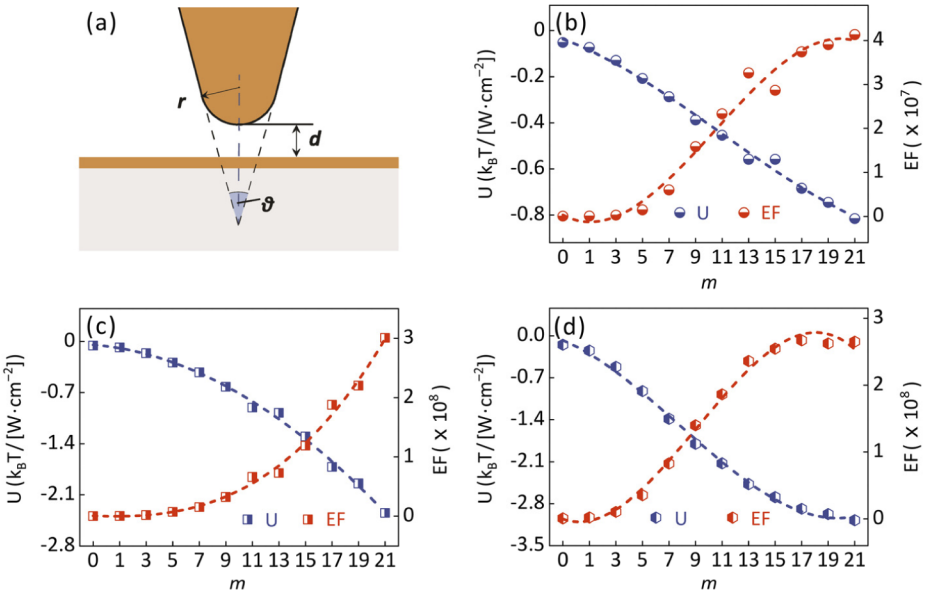

Fig. 6. Nonlinearity-modulated potential depths and Raman EFs of the system with different configurable parameters. (a) Graphical parameters of the configurable system. (b) $d = 10$ nm, (c) $r = 15$ nm, and (d) $\vartheta = 20°$. Other parameters are in accordance with Fig. 2.

Furthermore, there are still other parameters that may affect the results in an actual experiment. For instance, the electromagnetic absorption of the sample and solution will generate a certain amount of heat, and the resulting a thermal convection will reduce the stability of the optical trap. Here, fortunately, the heating can be suppressed to some extent for a pulsed excitation due to the temperature dissipation between pulses. Also, nonlinearities of the sample and solution are not taken into consideration here. But, because most dielectrics exhibit much weaker third-order nonlinearities than metallic materials, this simplification will not affect the conclusions. Moreover, due to strict coupling conditions, only a small portion of the incident light beam satisfies the critical angle of the surface plasmon excitation thus contributes to the formation of the gap plasmon in this configuration. To improve the utilization of the incident energy, many schemes have been proposed such as confining the beam into a narrow annulus satisfying the plasmonic

Optics EXPRESS

excitation [46,47]. In our previous work, it has been demonstrated that the field intensity and trapping stiffness can be 2.6 times enhanced in experiments with the optimized excitation method [48]. Therefore, it is reasonable to prospect that the nonlinearity-modulated single molecule trapping and enhanced Raman scattering system presented in this work will have higher trapping stiffness and detection sensitivity.

3. Conclusion

In summary, we proposed a nonlinearity-modulated single molecule trapping and enhanced Raman scattering system based on a bottom-illuminated TERS configuration. Due to the plasmonic hybridization and spatial confinement, a localized plasmon with high electromagnetic enhancement can be produced in the nanogap between the gold tip and substrate film, making it feasible to perform stable trapping and Raman detection at the single-molecule level. Due to the nonlinearity effect, intrinsic physical properties of the gold tip and substrate film can be proactively modulated; moreover, the optical force on the single molecule and its Raman scattering enhancement can response synchronously. The simulation results indicate that the nonlinearity brings a new modulation freedom for optical trapping and Raman spectroscopic detection and analysis. Furthermore, since plasmon excitation can respond on the timescales of a few femtoseconds [49,50], the method allows the plasmonic pulses to be used for monitoring ultrafast physical phenomena with nanometer spatial resolution and femtosecond time resolution. We believe that this work will not only provide a feasible all optical strategy for single molecule trapping and in-situ Raman detection, but also deliver important contributions towards comprehensive understanding of the ultra-small and ultra-fast light-matter interactions.

Funding. Guangdong Major Project of Basic and Applied Basic Research (2020B0301030009); National Natural Science Foundation of China (91750205, 61975128, 12074224, 12074268,); Leading Talents of Guangdong Province Program (00201505); Natural Science Foundation of Guangdong Province (2016A030312010, 2019TQ05X750); Shenzhen Peacock Plan (KQTD20170330110444030); Shenzhen Science and Technology Program (JCYJ20210324120403011, ZDSYS201703031605029, JCYJ20180305125418079).

Disclosures. The authors declare no conflicts of interest.

Data availability. Data underlying the results presented in this paper are not publicly available at this time but may be obtained from the authors upon reasonable request.

References

1. C. Zong, R. Premasiri, H. Lin, Y. Huang, C. Zhang, C. Yang, B. Ren, L. D. Ziegler, and J. Cheng, "Plasmon-enhanced stimulated Raman scattering microscopy with single-molecule detection sensitivity," Nat. Commun. **10**(1), 5318 (2019).
2. H. J. Park, S. Cho, M. Kim, and Y. S. Jung, "Carboxylic acid-functionalized, graphitic layer-coated three-dimensional SERS substrate for label-free analysis of Alzheimer's disease biomarkers," Nano Lett. **20**(4), 2576–2584 (2020).
3. E. K. Sackmann, A. L. Fulton, and D. J. Beebe, "The present and future role of microfluidics in biomedical research," Nature **507**(7491), 181–189 (2014).
4. H. Tan, H. Hu, L. Huang, and K. Qian, "Plasmonic tweezers for optical manipulation and biomedical applications," Analyst **145**(17), 5699–5712 (2020).
5. D. Gao, W. Ding, M. Nieto-Vesperinas, X. Ding, M. Rahman, T. Zhang, C. Lim, and C.-W. Qiu, "Optical manipulation from the microscale to the nanoscale: fundamentals, advances and prospects," Light: Sci. Appl. **6**(9), e17039 (2017).
6. M. L. Juan, M. Righini, and R. Quidant, "Plasmon nano-optical tweezers," Nat. Photon. **5**(6), 349–356 (2011).
7. Y. Zhang, C. Min, X. Dou, X. Wang, H. P. Urbach, M. G. Somekh, and X.-C. Yuan, "Plasmonic tweezers: for nanoscale optical trapping and beyond," Light: Sci. Appl. **10**(1), 59 (2021).
8. D. G. Kotsifaki and S. N. Chormaic, "Plasmonic optical tweezers based on nanostructures: fundamentals, advances and prospects," Nanophotonics **8**(7), 1227–1245 (2019).
9. J. Shen, J. Wang, C. Zhang, C. Min, H. Fang, L. Du, S. Zhu, and X.-C. Yuan, "Dynamic plasmonic tweezers enabled single-particle-film-system gap-mode Surface-enhanced Raman scattering," Appl. Phys. Lett. **103**(19), 191119 (2013).
10. J. J. Baumberg, J. Aizpurua, M. H. Mikkelsen, and D. R. Smith, "Extreme nanophotonics from ultrathin metallic gaps," Nat. Mater. **18**(7), 668–678 (2019).
11. H. Chen, Y. Zhang, Y. Dai, C. Min, S. Zhu, and X.-C. Yuan, "Facilitated tip-enhanced Raman scattering by focused gap-plasmon hybridization," Photonics Res. **8**(2), 103–109 (2020).

Optics EXPRESS

12. C. Pin, S. Ishida, G. Takahashi, K. Sudo, T. Fukaminato, and K. Sasaki, "Trapping and deposition of dye–molecule nanoparticles in the nanogap of a plasmonic antenna," ACS Omega **3**(5), 4878–4883 (2018).
13. C. Hong, S. Yang, and J. C. Ndukaife, "Stand-off trapping and manipulation of sub-10 nm objects and biomolecules using opto-thermo-electrohydrodynamic tweezers," Nat. Nanotechnol. **15**(11), 908–913 (2020).
14. Y. Chen, X. Serey, R. Sarkar, P. Chen, and D. Erickson, "Controlled photonic manipulation of proteins and other nanomaterials," Nano Lett. **12**(3), 1633–1637 (2012).
15. N. Kumar, B. M. Weckhuysen, A. J. Wain, and A. J. Pollard, "Nanoscale chemical imaging using tip-enhanced Raman spectroscopy," Nat. Protoc. **14**(4), 1169–1193 (2019).
16. E. Bailo and V. Deckert, "Tip-enhanced Raman scattering," Chem. Soc. Rev. **37**(5), 921–930 (2008).
17. F. Lu, W. Zhang, M. Liu, L. Zhang, and T. Mei, "Tip-based plasmonic nanofocusing: vector field engineering and background elimination," J. Sel. Top. Quant. **27**(1), 4600512 (2021).
18. Z. Man, Z. Xi, X. Yuan, R. E. Burge, and H. P. Urbach, "Dual coaxial longitudinal polarization vortex structures," Phys. Rev. Lett. **124**(10), 103901 (2020).
19. L. Long, J. Chen, H. Yu, and Z.-Y. Li, "Strong optical force of a molecule enabled by the plasmonic nanogap hot spot in a tip-enhanced Raman spectroscopy system," Photonics Res. **8**(10), 1573–1579 (2020).
20. J. Zhang, F. Lu, W. Zhang, W. Yu, W. Zhu, M. Premaratne, T. Mei, F. Xiao, and J. Zhao, "Optical trapping of single nano-size particles using a plasmonic nanocavity," J. Phys.: Condens. Matter **32**(47), 475301 (2020).
21. A. B. Zrimsek, N. Chiang, M. Mattei, S. Zaleski, M. O. McAnally, C. T. Chapman, A.-I. Henry, G. C. Schatz, and R. P. Van Duyne, "Single-molecule chemistry with surface-and tip-enhanced Raman spectroscopy," Chem. Rev. **117**(11), 7583–7613 (2017).
22. P. Liu, D. V. Chulhai, and L. Jensen, "Single-molecule imaging using atomistic near-field tip-enhanced Raman spectroscopy," ACS Nano **11**(5), 5094–5102 (2017).
23. L. Gong, B. Gu, G. Rui, Y. Cui, Z. Zhu, and Q. Zhan, "Optical forces of focused femtosecond laser pulses on nonlinear optical Rayleigh particles," Photonics Res. **6**(2), 138–143 (2018).
24. Y. Jiang, T. Narushima, and H. Okamoto, "Nonlinear optical effects in trapping nanoparticles with femtosecond pulses," Nat. Phys. **6**(12), 1005–1009 (2010).
25. C. Min, Z. Shen, J. Shen, Y. Zhang, H. Fang, G. Yuan, L. Du, S. Zhu, T. Lei, and X.-C. Yuan, "Focused plasmonic trapping of metallic particles," Nat. Commun. **4**(1), 2891 (2013).
26. Y. Wang, B. Zhao, C. Min, Y. Zhang, J. Yang, C. Guo, and X.-C. Yuan, "Research progress of femtosecond surface plasmon polariton," Chinese Phys. B **29**(2), 027302 (2020).
27. Z. L. Sámson, P. Horak, K. F. MacDonald, and N. I. Zheludev, "Femtosecond surface plasmon pulse propagation," Opt. Lett. **36**(2), 250–252 (2011).
28. G. Rosenblatt, B. Simkhovich, G. Bartal, and M. Orenstein, "Nonmodal plasmonics: Controlling the forced optical response of nanostructures," Phys. Rev. X **10**(1), 011071 (2020).
29. R. W. Boyd, Z. Shi, and I. L. De, "The third-order nonlinear optical susceptibility of gold," Opt. Commun. **326**, 74–79 (2014).
30. S. Albaladejo, M. I. Marqués, M. Laroche, and J. J. Sáenz, "Scattering forces from the curl of the spin angular momentum of a light field," Phys. Rev. Lett. **102**(11), 113602 (2009).
31. Q. Zhan, "Trapping metallic Rayleigh particles with radial polarization," Opt. Express **12**(15), 3377–3382 (2004).
32. T. Simonson and C. L. Brooks, "Charge screening and the dielectric constant of proteins: insights from molecular dynamics," J. Am. Chem. Soc. **118**(35), 8452–8458 (1996).
33. B. T. Draine, "The discrete-dipole approximation and its application to interstellar graphite grains," Astrophys. J. **333**, 848–872 (1988).
34. C. F. Bohren and D. R. Huffman, *Absorption and scattering of light by small particles* (John Wiley & Sons, 2008).
35. A. A. Saleh and J. A. Dionne, "Toward efficient optical trapping of sub-10-nm particles with coaxial plasmonic apertures," Nano Lett. **12**(11), 5581–5586 (2012).
36. O. M. Maragò, P. H. Jones, P. G. Gucciardi, G. Volpe, and A. C. Ferrari, "Optical trapping and manipulation of nanostructures," Nat. Nanotechnol. **8**(11), 807–819 (2013).
37. C. Zhan, G. Wang, J. Yi, J. Wei, Z. Li, Z. Chen, J. Shi, Y. Yang, W. Hong, and Z.-Q. Tian, "Single-molecule plasmonic optical trapping," Matter **3**(4), 1350–1360 (2020).
38. H. Xu and M. Käll, "Surface-plasmon-enhanced optical forces in silver nanoaggregates," Phys. Rev. Lett. **89**(24), 246802 (2002).
39. N. Calander and M. Willander, "Optical trapping of single fluorescent molecules at the detection spots of nanoprobes," Phys. Rev. Lett. **89**(14), 143603 (2002).
40. Y. Kitahama, M. Funaoka, and Y. Ozaki, "Plasmon-enhanced optical tweezers for single molecules on and near a colloidal silver nanoaggregate," J. Phys. Chem. C **123**(29), 18001–18006 (2019).
41. Y. Tsuboi, T. Shoji, N. Kitamura, M. Takase, K. Murakoshi, Y. Mizumoto, and H. Ishihara, "Optical trapping of quantum dots based on gap-mode-excitation of localized surface plasmon," J. Phys. Chem. Lett. **1**(15), 2327–2333 (2010).
42. X. Wang, S. Huang, S. Hu, S. Yan, and B. Ren, "Fundamental understanding and applications of plasmon-enhanced Raman spectroscopy," Nat. Rev. Phys. **2**(5), 253–271 (2020).

Optics EXPRESS

43. B. Wang, C. Zhao, H. Lu, T. Zou, S. C. Singh, Z. Yu, C. Yao, X. Zheng, J. Xing, and Y. Zou, "SERS study on the synergistic effects of electric field enhancement and charge transfer in an Ag2S quantum dots/plasmonic bowtie nanoantenna composite system," Photonics Res. **8**(4), 548–563 (2020).
44. S. Kawata and V. M. Shalaev, *Tip enhancement* (Elsevier, 2011).
45. Y. Yu, T. Xiao, Y. Wu, W. Li, Q. Zeng, L. Long, and Z.-Y. Li, "Roadmap for single-molecule surface-enhanced Raman spectroscopy," Adv. Photonics **2**(1), 014002 (2020).
46. A. S. Ostrovsky, C. R. Parrao, and V. Arrizón, "Generation of the "perfect" optical vortex using a liquid-crystal spatial light modulator," Opt. Lett. **38**(4), 534–536 (2013).
47. J. Yu, C. Miao, J. Wu, and C. Zhou, "Circular Dammann gratings for enhanced control of the ring profile of perfect optical vortices," Photonics Res. **8**(5), 648–658 (2020).
48. X. Wang, Y. Zhang, Y. Dai, C. Min, and X.-C. Yuan, "Enhancing plasmonic trapping with a perfect radially polarized beam," Photonics Res. **6**(9), 847–852 (2018).
49. M. I. Stockman, "Nanoplasmonics: past, present, and glimpse into future," Opt. Express **19**(22), 22029–22106 (2011).
50. G. Spektor, D. Kilbane, A. Mahro, B. Frank, S. Ristok, L. Gal, P. Kahl, D. Podbiel, S. Mathias, and H. Giessen, "Revealing the subfemtosecond dynamics of orbital angular momentum in nanoplasmonic vortices," Science **355**(6330), 1187–1191 (2017).